

Soil and Glass Surface Photodegradation of Etofenprox under Simulated California Rice Growing Conditions

Martice Vasquez,^{*,†} Thomas Cahill,[‡] and Ronald Tjeerdema[†]

[†]Department of Environmental Toxicology, College of Agriculture and Environmental Sciences, University of California, One Shields Avenue, Davis, California 95616-8588, United States

[‡]Division of Mathematical and Natural Sciences, Arizona State University at the West Campus, P.O. Box 37100, Phoenix, Arizona, 85069

 Supporting Information

ABSTRACT: Photolysis is an important degradation process to consider when evaluating a pesticide's persistence in a rice field environment. To simulate both nonflooded and flooded California rice field conditions, the photolytic degradation of etofenprox, an ether pyrethroid, was characterized on an air-dried rice soil and a flooded rice soil surface by determination of its half-life ($t_{1/2}$), dissipation rate constant (k) and identification and quantitation of degradation products using LC/MS/MS. Photodegradation was also characterized on a glass surface alone to rule out confounding soil factors. Measured photolytic dissipation rates were used as input parameters into a multimedia environmental fate model to predict etofenprox persistence in a rice field environment. Photolytic degradation proceeded at a faster rate (0.23/day, $t_{1/2} = 3.0$ days) on the flooded soil surface compared to the air-dried surface (0.039/day, $t_{1/2} = 18$ days). Etofenprox degradation occurred relatively quickly on the glass surface (3.1/day, $t_{1/2} = 0.23$ days or 5.5 h) compared to both flooded and air-dried soil layers. Oxidation of the ether moiety to the ester was the major product on all surfaces (max % yield range = 0.2 ± 0.1% to 9.3 ± 2.3%). The hydroxylation product at the 4' position of the phenoxy phenyl ring was detected on all surfaces (max % yield range = 0.2 ± 0.1% to 4.1 ± 1.0%). The air-dried soil surface did not contain detectable residues of the ester cleavage product, whereas it was quantitated on the flooded soil (max % yield = 0.6 ± 0.3%) and glass surface (max % yield = 3.6 ± 0.6%). Dissipation of the insecticide in dark controls was significantly different ($p < 0.05$) compared to the light-exposed surfaces indicating that degradation was by photolysis. Laboratory studies and fate model predictions suggest photolysis will be an important process in the overall degradation of etofenprox in a rice field environment.

KEYWORDS: insecticides, pyrethroids, etofenprox, photolytic degradation, soil surface, level IV fugacity model

INTRODUCTION

Over 534,000 acres of rice were planted in the Sacramento Valley in 2008.¹ Pest management is essential to maintain rice crop health and yields, and chemical agents used to do so must be well understood to ensure chemical residues do not pose risk to nontarget organisms and environments once applied. California rice farmers are interested in using the pyrethroid insecticide, etofenprox, 1 (Figure 1), for rice water weevil control. Etofenprox is currently undergoing registration for use in California rice culture. It is important to understand how etofenprox will move and transform in the rice field environment for effective residue management and prevention of offsite movement into the Sacramento River. Pyrethroids in general are increasing in usage as a result of low mammalian toxicity; however, they are highly toxic to aquatic species,² and thus, their movement and transformation in the environment must be understood to minimize risk.

Degradation via sunlight can be a major dissipation pathway for pesticides leading to diminished persistence in the air, water and soil surface environments. Permethrin, an ester pyrethroid, has been shown to be more photolabile than etofenprox, an ether pyrethroid.³ This study did not include water as a solvent due to the extreme insolubility of etofenprox, and thus a completely aqueous photolytic study is not practical. Our previous work^{4,5} suggests that etofenprox will rapidly dissipate from water and sorb to soils where it can be degraded by soil microbes, slowly under anaerobic conditions. Photolytic degradation of soil-

bound residues may also contribute to the overall dissipation from a rice field. Due to periods of flooded and nonflooded field conditions in California rice culture, we have characterized the photoinduced degradation of etofenprox in a bound state on an air-dried and flooded California rice soil surface, under sterile conditions. The glass surface model is a good first approach to investigate surface photodegradation of pesticides, since soil humic substances are not able to act as a filter, photosensitizer, quencher or solubilizing agent.⁶ To rule out these complicating factors, etofenprox photolytic degradation also was examined on a glass (mineral) surface. This investigation aims to describe the photolytic degradation of surface sorbed etofenprox by determination of the dissipation rate constant (k), the half-life ($t_{1/2}$) of etofenprox and identification and quantitation of photoinduced degradation products under simulated California summer rice field conditions. Rate constants were used as inputs into a multimedia environmental fate model (level IV fugacity model) to compare fate, transport and persistence of etofenprox and malathion, an organophosphorus insecticide used in rice but having a greater aqueous solubility (145 mg/L) relative to etofenprox (0.0225 mg/L), in a simulated field environment.

Received: March 2, 2011

Accepted: June 15, 2011

Revised: June 15, 2011

Published: June 15, 2011

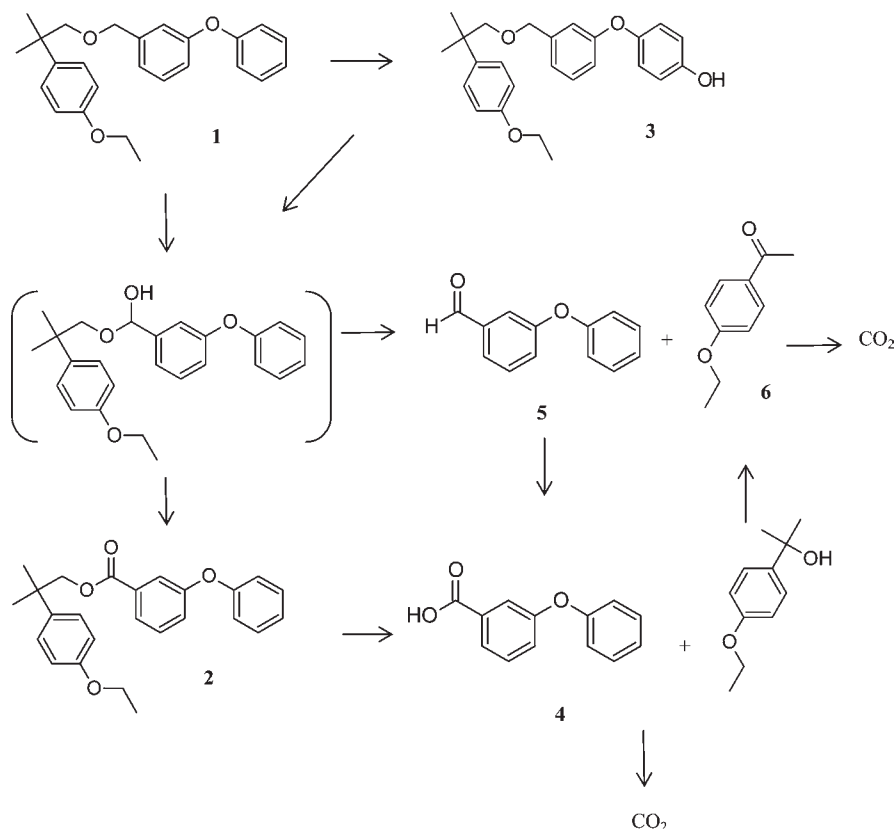


Figure 1. Proposed photolytic degradation pathway of etofenprox.

MATERIALS AND METHODS

Chemicals. Etofenprox (2-(4-ethoxyphenyl)-2-methylpropyl 3-phenoxybenzyl ether; 1), 2-(4-ethoxyphenyl)-2-methylpropyl 3-phenoxybenzoate (2), and 2-(4-ethoxyphenyl)-2-methylpropyl 3-hydroxybenzyl ether (3) were supplied gratis by Mitsui Co. (Tokyo, Japan). Sodium azide and 3-phenoxybenzoic acid (4) were purchased from Sigma (St. Louis, MO), while Optima hexane, Optima acetone, Optima methanol and HPLC-grade water and acetonitrile were purchased from Fisher Scientific (Hampton, NH). Stock solutions of etofenprox were prepared in methanol.

Soil Collection and Characterization. Rice field soil was collected from the UC Rice Experiment Station (Biggs, CA) in June 2010; it was air-dried and ground to pass through a 2 mm sieve, and stored at 4 °C until use. The soil was characterized by the Division of Agriculture and Natural Resources (ANR) Analytical Laboratory at the University of California, Davis.⁷ Briefly, particle size (22% sand, 32% silt, 46% clay content) was determined using the hydrometer method;⁸ organic matter (0.54%) was analyzed using the Walkley–Black method with spectrophotometric detection.⁹ The soil is classified as an Esquon-Neerdobe thermic clay loam,¹⁰ representative of typical California rice growing soil.

Soil Layer Preparation. Twenty grams of soil was spread evenly into a Pyrex Petri dish (100 mm diameter) yielding a 2 mm thick soil layer as described previously.¹¹ All soil plates were autoclaved 3 times to remove microbial activity and were kept covered during the experiment with Pyrex lids. Plates used to simulate soil surface photolysis in a flooded field maintained a 4 mm water (autoclaved) layer. A ratio of 2:1 (water: soil) was used to represent the shallow depth of a flooded rice field. Since the depth of light penetration in soil is estimated at 0.5 mm,¹¹ the soil layer thickness (2 mm) is considered adequate to represent the photolytic zone in the field. Etofenprox (150 µg in 250 µL of methanol)

was added evenly to the soil or water surface for air-dried soil samples or flooded soil samples, respectively, as well as to plates without soil. Plates were kept for 24 h in the dark to allow for solvent evaporation before the start of the photoperiod in the photoreactor. The start of the photoperiod was taken as time zero and represented the 100% level of initial etofenprox.

Photoreactor and Exposures. Four (8 W) broad UV (300 ± 50 nm) spectrum lights (Southern New England, Branford, CT) were mounted 270 mm directly above the soil surface. The photoreactor was wrapped with reflective paneling to prevent light escaping. Pyrex covers were placed on Petri dishes to filter light below the solar cutoff of 295 nm. The intensity of light (7.4 W/m²) exposure at the soil surface was measured with a portable radiometer, and was comparable to the intensity of sunlight in a typical California rice field during the summer growing season (noon, June). For comparison, a radiometer reading of 11.4 W/m² was measured on the roof of Meyer Hall at the University of California, Davis, at noon on June 30, 2010. The temperature (28 °C) in the photoreactor was maintained with 2 cooling fans and exhaust ducts. Control samples were placed in the photoreactor but covered with aluminum foil to prevent exposure to the simulated sunlight. All photoexposed and dark control samples were prepared in triplicate for each time interval (0, 1, 2, 3, 4, 5, 7, 10, 15, 20, 29 days or 0, 1, 2, 3, 5, 8, 15, 24, 48, 72 h for plate only experiment). At each interval, Petri dishes were solvent extracted and the extracts were collected and analyzed for etofenprox and photoproducts by LC/MS/MS.

Extraction and Analysis. Soil plate contents were quantitatively transferred to 300 mL amber bottles with 50 mL of acetone and were placed on a platform shaker at 135 rpm overnight. Acetone (chosen for intermediate polarity and broad extraction range) extracts were vacuum filtered, and the soil cake was washed with acetone. The acetone extract was blown down to 10 mL under nitrogen gas at room temperature, and 30 mL of water was added for air-dried soil extracts and 10 mL for

flooded soil extracts. The acetone–water extracts were liquid/liquid extracted with hexane (3×10 mL) and brought to dryness under nitrogen gas at room temperature. The residues were dissolved in 2 mL of 40:60 acetonitrile:water, filtered ($0.45 \mu\text{m}$) and then analyzed by LC/MS/MS. Residues from plates without soil were extracted by addition of acetone (3×5 mL) to the plate followed by quantitative transfer of the acetone extract to an evaporation vessel. The extract was brought to dryness under nitrogen gas, and the residues were dissolved in 2 mL of 40:60 acetonitrile:water, filtered ($0.45 \mu\text{m}$) and then analyzed by LC/MS/MS.

Analysis of etofenprox and photoproducts was described previously.⁵ Briefly, LC/MS/MS analysis was performed using a HP 1100 HPLC (Palo Alto, CA) coupled to an Applied Biosystems Sciex 2000 triple quadrupole LC/MS/MS (South San Francisco, CA) using electrospray ionization (ESI). The chromatographic column used was a 100 mm \times 2.1 mm i.d., $5 \mu\text{m}$, Titan C₁₈ analytical column (Peeke Scientific, Sunnyvale, CA), with a flow rate of 0.25 mL/min and a 40 μL injection volume. The solvent gradient profile for **1–3** was as follows: solvent A, acetonitrile (0.1% ammonium acetate); solvent B, water (0.1% ammonium acetate); 0–4.5 min, 40% A:60% B; 4.5–10 min, 95% A:5% B; 11–20 min, 40% A:60% B. The gradient profile for **4** determination was as follows: solvent A, acetonitrile (0.1% acetic acid); solvent B, water (0.1% acetic acid); 0–6 min, 20% A:80% B; 6–15 min 40% A:60% B; 15–20 min 20% A:80% B.

Compounds **1–4** were quantified in multiple reaction monitoring mode (MRM) against a second order calibration curve generated in Analyst software version 1.2.4 using matrix matched standards. Mass transitions monitored were as follows: $m/z 394 \rightarrow 177$, $m/z 408 \rightarrow 177$, $m/z 410 \rightarrow 177$ and $m/z 203 \rightarrow 93$, for **1–4**, respectively. Positive ionization mode was used for **1–3** and negative mode for **4**. Collision energies and declustering potentials were optimized for each compound. Prior to sample injection for **1** quantitation, extracts were diluted (1/100 or 1/200) with mobile phase to produce an area response within the calibration range. The instrument detection limit was 0.01 mg/L, 0.05 mg/L, 0.05 mg/L and 0.05 mg/L for **1–4** respectively, as determined by multiplying 3 times the standard deviation of replicate injections of low level standards. Target analyte soil extraction efficiencies at a 3 mg/kg spike level were $95.6\% \pm 3.5\%$, $92.4\% \pm 2.8\%$, $89.6\% \pm 3.3\%$, and $69.7\% \pm 6.0\%$, for **1–4**, respectively. Soil extraction efficiencies at a 0.5 mg/kg spike level were $80.8\% \pm 3.7\%$, $74.0\% \pm 4.0\%$, $73.2\% \pm 5.5\%$, and $51.2\% \pm 4.8\%$, for **1–4**, respectively.

Data Analysis. Photodegradation rate constants were calculated based on first order kinetics where the rate constant (k) is calculated from the equation:

$$C_t = C_0 e^{-kt} \quad (1)$$

and C_0 is the initial concentration ($\mu\text{g/g}$ or $\mu\text{g/cm}^2$) of etofenprox, C_t is the concentration ($\mu\text{g/g}$ or $\mu\text{g/cm}^2$) at time t (day) and k is the first order degradation rate constant. The half-life ($t_{1/2}$) is calculated according to the equation

$$t_{1/2} = (\ln 2)/k \quad (2)$$

One-way ANOVA was used for comparison of degradation rates between control (dark) and light exposed soils.

Level IV High Resolution Fugacity Model. A level I fugacity model was previously used to describe the partitioning of etofenprox in a defined rice field environment.⁴ In order to incorporate chemical reaction and transport processes in the partitioning model, a more complex fugacity based multimedia fate model (level IV high resolution) has been constructed, based on previously described models.¹² This model is a useful tool to estimate the mass distribution and residence time of a chemical within each environmental compartment (air, water, soil and sediment) and subcompartment (i.e., sediment layer 1 (surface),

Table 1. Pseudo First Order Kinetic Summary of Etofenprox Photoinduced Dissipation on an Air-Dried Soil, a Flooded Soil and a Glass Surface at 28 ± 1 °C

| kinetic parameters | k (per days) | $t_{1/2}$ (days) | r^2 |
|--------------------------|----------------|------------------|-------|
| air-dried soil | 0.039 | 18 | 0.97 |
| flooded soil (0–10 days) | 0.23 | 3.0 | 0.95 |
| glass plate (0–1 day) | 3.1 | 0.23 | 0.97 |

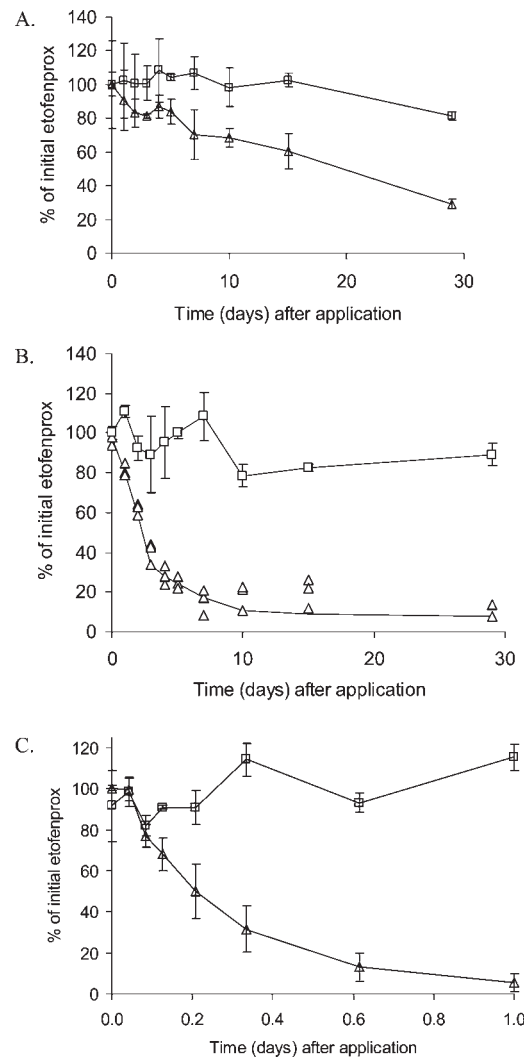


Figure 2. Decrease in the percent applied mass of etofenprox on an air-dried soil surface (A), a flooded soil surface (B) and a glass surface (C) at 28 °C under simulated sunlight. Points represent the mean \pm SD ($n=3$) for dark control (\square) and light exposed (Δ) surfaces except for the light exposed (Δ) flooded soil surface (B), where points represent individual experimental replicates.

sediment layer 2 (middle) and sediment layer 3 (lower)) in a dynamic rice field environment. Assumptions of the level IV model include dynamic, nonequilibrium conditions within and between compartments, but the chemical is presumed to be well mixed within each subcompartment.¹² The high resolution level IV model further subdivides the atmosphere, aerosol, soil and sediment into 3 subcompartments or layers. The depth, volume and density of each compartment and subcompartment are given in the Supporting Information. A complete model description and input parameter data can be found in

Cahill and MacKay.¹² This model accounts for inter- and intramedia transport as well as transformation processes such as reaction, advection and diffusion. Transport parameters, such as the rate of molecular diffusivity of a chemical in air and water, are defined. Mass transfer coefficients are included to describe the rate of chemical movement across compartment and subcompartment boundary layers. Sediment deposition, resuspension and burial rates are also built into the model. Chemical reaction rates for each compartment and subcompartment are provided in the Supporting Information. Previously determined microbial degradation rates of etofenprox under both flooded and nonflooded soil conditions⁵ were combined with the photodegradation rates determined in this study to estimate the overall degradation in each compartment or subcompartment. Where degradation data was lacking, the most relevant measured degradation value for the respective compartment was used.

This model simulates a one time chemical pulse to a defined rice field environment. The simulation begins with an etofenprox application made aerially to a 247 acre area (90% of acreage flooded; flooded soil is sediment in model), representative of a large family rice farm.¹³ Model inputs, such as environmental parameters, chemical properties and reaction rates, are summarized in the Supporting Information. The field is assumed to have no to little vegetation density, as etofenprox is applied one to seven days after field flooding and seeding.¹⁴ Air and water parcel residence times were set to 12 h and 30 days, respectively. For comparison, the fate and persistence of malathion, an organophosphorus insecticide currently used in California rice culture, was also predicted using the level IV fugacity model. The California Department of Pesticide Regulation reported that 1.41 lb/acre¹⁵ of malathion was applied to rice fields in 2008, and this value was used as an approximate application rate for the model; the maximum application rate of 0.3 lb/acre¹⁴ was the etofenprox input amount. The fate and persistence was modeled over 100 days.

RESULTS AND DISCUSSION

Comparison of Soil Surface Degradation Rates and Half-Lives. The pseudo first order photoinduced degradation rate constants of etofenprox are presented in Table 1. As shown in Figure 2, degradation proceeded at a faster rate (0.23/day, $t_{1/2} = 3.0$ days) on the flooded soil surface compared to the air-dried surface (0.039/day, $t_{1/2} = 18$ days). After 10 days of light exposure, the flooded soil degradation curve based on replicate averages ($n = 3$) began to deviate from the first order kinetic model. Poor fit was likely due to experimental error at the later time points, as most of the applied mass has dissipated (<15%) after 10 days. Evaluation of dissipation from the flooded soil surface on an individual replicate basis revealed a set of points representing a reasonable first order decay process throughout the photoperiod (Figure 2), yet the kinetics were modeled over the 10 day period for the flooded soil surface. After 29 days, 29.1% of the initial applied mass remained in the air-dried soil (Figure 2). Dissipation of the insecticide in dark controls was significantly different ($p < 0.05$) compared to the light exposed surfaces, indicating that degradation was by photolysis.

Increased soil surface moisture levels, 75% moisture holding capacity (MHC) versus air-dried, have been shown to increase esfenvalerate photodegradation rates initially, but overall half-lives were not statistically different.¹¹ The highly sorptive nature of pyrethroids is suggested to result in little movement into the subsurface soil layers with residues remaining in the photolytic zone (0.5 mm) whether there is moisture present or not.¹¹ It is within this photic zone that direct photolysis is thought to occur.¹⁶ The experimental design of a 2 mm soil layer is

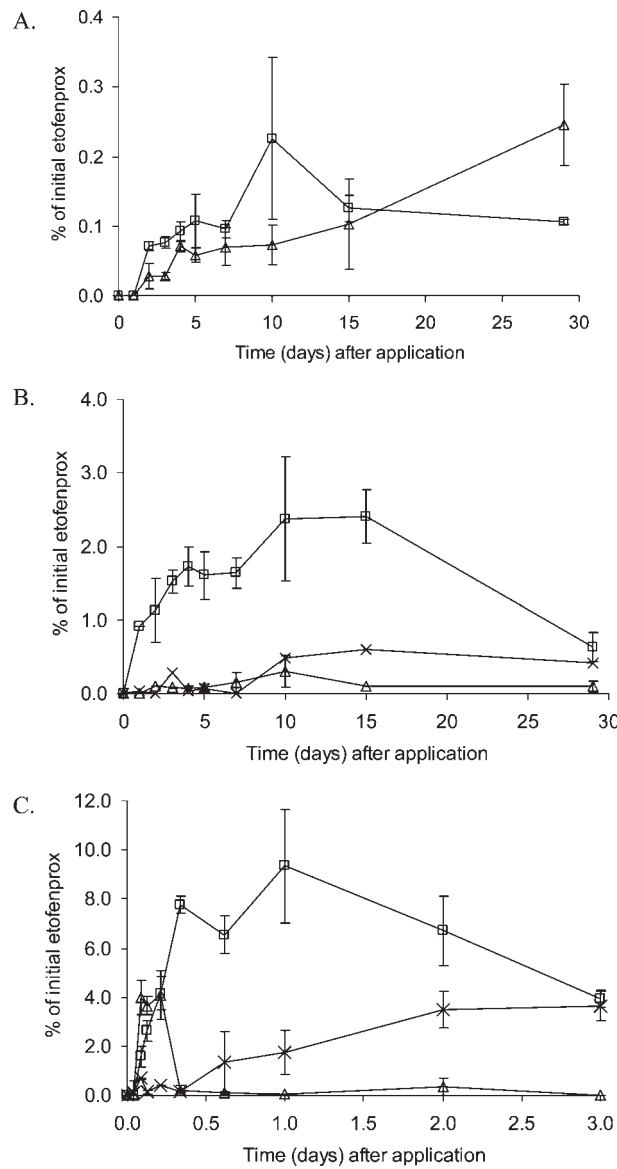


Figure 3. Major photoinduced transformation products of etofenprox on an air-dried soil surface (A), a flooded soil surface (B) and a glass surface (C) under simulated sunlight at 28 °C: compound 3 (Δ), compound 2 (□) and compound 4 (×). Points represent mean \pm SD ($n = 3$).

considered adequate to represent the maximum light penetrating depth of sunlight in a bare rice field if the photic zone is considered 0.5 mm.

In a flooded soil system, it is possible the thin water layer can aid the diffusion of reactive species resulting in increased rates of indirect photoinduced chemical degradation compared to an air-dried soil surface. The water layer may contribute to a greater concentration of reactive species in the system. Reactive species, such as dissolved organic matter, dissolved oxygen, and nitrates in the aqueous layer and in the soil pore water, could enhance photoinduced degradation compared to an air-dried soil. Species such as hydroxyl radical are suggested to be generated by metal oxides and by excitation of humic substances in water and soils.^{6,17} As a result, the flooded soil system is more complex than the air-dried soil system due to the presence of the aqueous

Table 2. Maximum Yield of Detected Photoproducts and Overall Mass Balance (% \pm SD^a of Initial Applied Mass of Etofenprox)

| surface | max % 2 | max % 3 | max % 4 | % etofenprox untransformed | % initial mass recovered |
|----------------|---------------|---------------|-----------------|----------------------------|--------------------------|
| air-dried soil | 0.2 \pm 0.1 | 0.2 \pm 0.1 | nd ^b | 29.1 \pm 2.9 | 29.5 \pm 3.1 |
| flooded soil | 2.4 \pm 0.4 | 0.3 \pm 0.2 | 0.6 \pm 0.3 | 15.0 \pm 3.3 | 18.3 \pm 4.2 |
| glass plate | 9.3 \pm 2.3 | 4.1 \pm 1.0 | 3.6 \pm 0.6 | 1.8 \pm 0.6 | 18.8 \pm 7.5 |

^a $n = 3$ (Figure 3) at 28 \pm 1 °C. ^b Not detected.

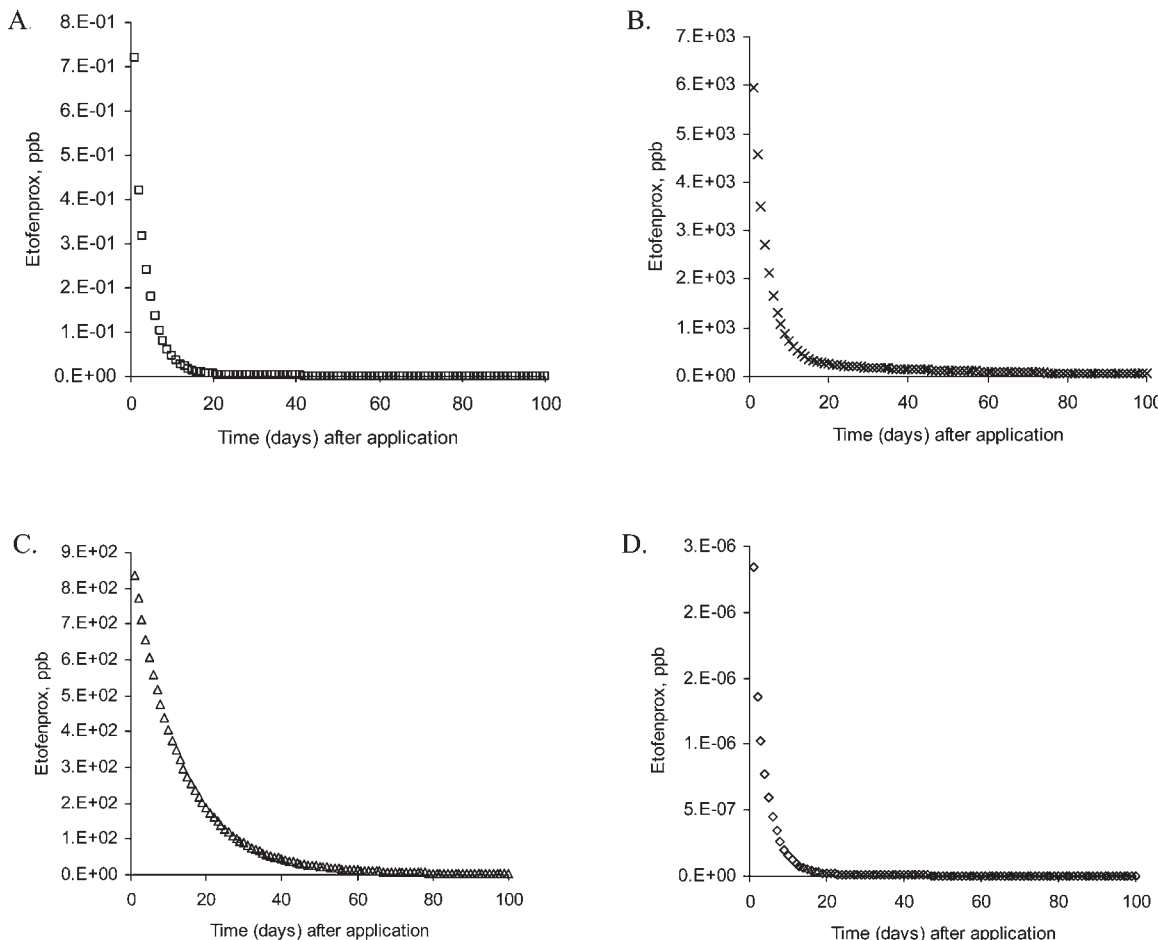


Figure 4. Predicted dissipation profile of etofenprox in water (A), sediment (B), soil (C) and air (D) using a level IV fugacity model over 100 days.

layer. It is suggested that a similar complex condition would prevail in a flooded field environment as under laboratory conditions, although a deeper water layer in the field may decrease light penetration at the soil surface.

Photodegradation from Glass Surface. The degradation kinetics of etofenprox applied to the glass surface alone is presented in Table 1. As shown in Figure 2, etofenprox degradation occurred relatively quickly on the glass surface (3.1/day, $t_{1/2} = 0.23$ days or 5.5 h) compared to both flooded and air-dried soil layers. After 3 days of light exposure, 2% of the initial applied mass of etofenprox remained. A similar photodegradation $t_{1/2}$ of 4.9 h was reported previously for etofenprox on a glass surface.¹⁸

The potential for the adsorbed pesticide to either absorb light directly or come into contact with a reactive species is less complicated by the absence of the soil layer. It is not possible to distinguish between direct photolysis of etofenprox on the glass surface and a glass surface catalyzed reaction. Without the humic substances in the soil to act as a filter, photosensitizer, quencher

or solubilizing agent, the glass surface model is a good first approach to investigate surface photodegradation of pesticides.⁶

Identification and Quantification of Degradation Products.

Three photoinduced degradation products were identified: (i) 2, the product of oxidation of the ether to the ester; (ii) 3, via hydroxylation at the 4' carbon of the phenoxy phenyl ring; (iii) 4, the ester cleavage product of 2 (Figure 1); maximum yields formed on each surface type are presented in Figure 3 and Table 2. The major product on all surfaces was 2, with the least overall amount of photoproduct formation on the air-dried soil. The air-dried soil surface did not contain detectable residues of 4, whereas 4 was quantitated on the flooded soil and glass surface. This is possibly a result of the higher levels of 2 produced on each respective surface which yields a greater concentration of reactant available for 4 formation. Photolytic ester cleavage of other pyrethroids as thin films has been reported previously, as well as a mixture of major and minor photoproducts,^{3,18} not targeted in this analysis. Compound 3 was quantifiable on all surfaces, with

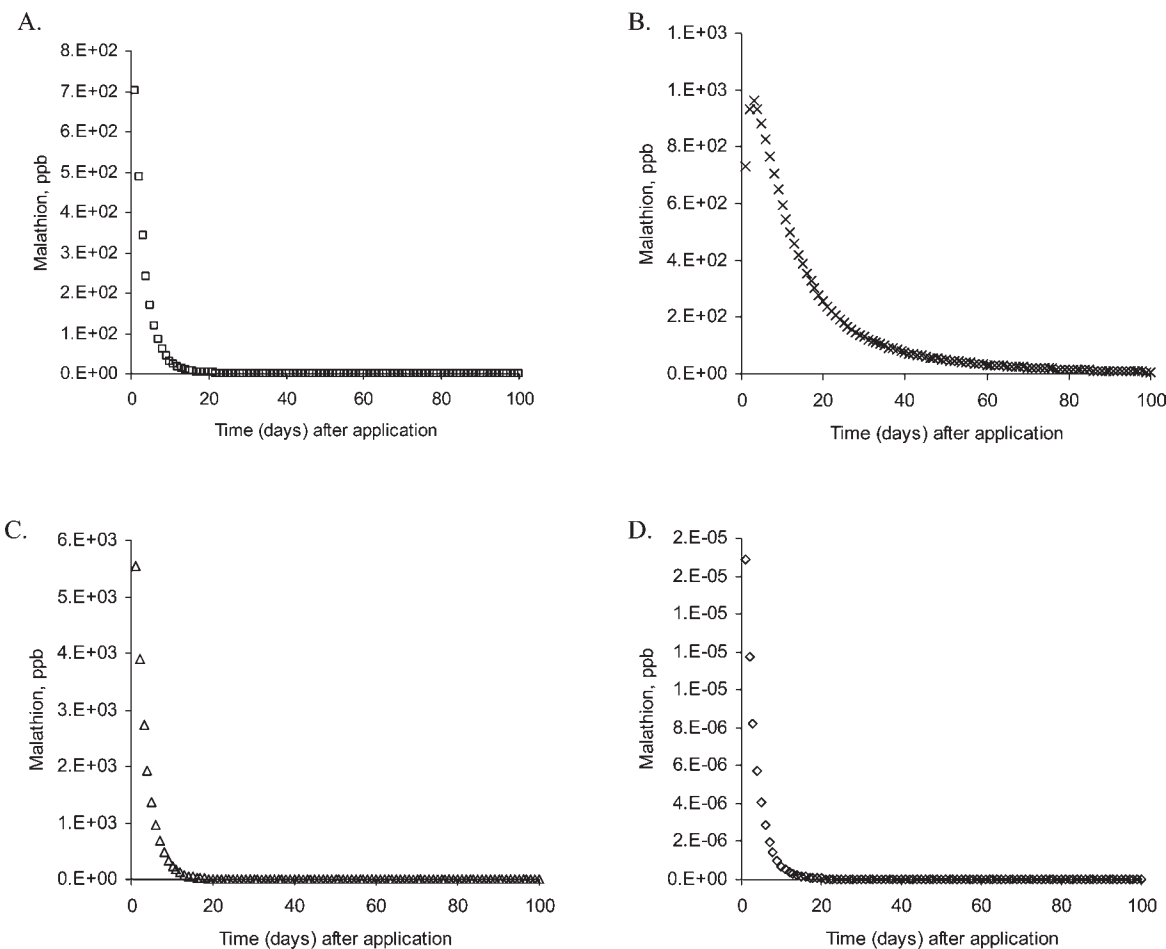


Figure 5. Predicted dissipation profile of malathion in water (A), sediment (B), soil (C) and air (D) using a level IV fugacity model over 100 days.

maximum yields similar to those of **4** on the flooded soil and glass surfaces. Unidentified products with the same mass transition as **3** but different retention times were seen mainly on the glass plate. The overall mass balance of etofenprox and its photoproducts ranged from $18.3\% \pm 4.2\%$ to $29.5\% \pm 3.1\%$ (Table 2). A combination of mineralization and targeted analysis may have contributed to the low mass balance (Table 2). A previous study identified compound **2** as the major etofenprox photoproduct from an irradiated glass surface but identified 3-phenoxybenzaldehyde, **5** (Figure 1), and 4'-ethoxyacetophenone, **6** (Figure 1), as the second and third most abundant photoproducts.¹⁸ In a similar study, **3** and **6** were not identified and **5** was considered a minor product.³ These previous studies only identified photoproducts and did not quantify yields.^{3,18} Photoproducts **5** and **6** were not targeted in our analysis, possibly contributing to the low mass balance. Analytical losses during sample extraction may have also contributed to the low mass balance. Analyte loss was greater at lower concentrations and can be expected to be at least a 30% loss at soil concentrations less than 0.5 mg/kg based on method validation data. A cleanup procedure was not required for the glass plate samples (liquid/liquid extraction) and could have resulted in increased photoproduct recovery compared to the soil samples. This is possibly a result of the highly sorptive nature of etofenprox and its degradation products. Direct injection of the water layer could have been possible if concentrations were above analytical detection limits.

The proposed photolytic degradation pathway for etofenprox is presented in Figure 1. A similar partial pathway has been proposed, but this pathway does not include **3** as a product as seen in this study.^{3,18} Photoproduct **2** has been identified previously as the major photodegradation product of etofenprox from an irradiated glass surface, similar to this study.^{3,18} As discussed previously in terms of mass balance, the majority of the unrecovred mass fraction of etofenprox on the glass plate is presumed to be lost as unidentified photoproducts and as CO₂. The dissipation curve implies complete degradation and transformation. A mixture of other major and minor oxidative photoproducts have been identified^{3,18} suggesting a complex progression of oxidative reactions. The photodegradation of **4** has been characterized previously resulting in oxidative mineralization via hydroxybenzoic acid intermediates.¹⁹

Photoinduced soil surface degradation of pesticides is expected to act in conjunction with soil microbes to ultimately degrade and transform applied chemicals. Photolytic processes are reported to be more important than microbial in the degradation of esfenvalerate on soil surfaces.²⁰ Similar microbial degradation products were identified under both aerobic and anaerobic soil incubations of etofenprox,⁵ suggesting a similar degradation pathway by different mechanisms, whether under abiotic or biotic control. The main photodegradation product, **2**, has been shown to lack insecticidal activity on houseflies,¹⁸ yet little data on the toxicity of the transformation products to environmental receptors is

available. Endocrine disruption by 4 has been reported in a yeast based assay,²¹ yet estrogenic activity was not exhibited in a breast cancer cell line or Sprague–Dawley rats.²²

High Resolution Multimedia Fugacity Model (Level IV). The predicted dissipation profile of etofenprox (Figure 4) and malathion (Figure 5) is presented for each environmental compartment: water, sediment, soil and air. Following etofenprox application, concentrations in all compartments decreased (Figure 4). Very low air concentrations compared to other compartments suggest little mass is predicted to volatilize after application or from the field water (Figure 4) over the 100 day simulation. Sediment concentrations remain greatest in the surface subcompartment of the sediment (sediment layer 1) until the majority of the chemical is degraded by a combination of photolytic and microbial degradation processes. Sediment layer 1 residues decrease over time to concentrations less than the underlying layers but only after the majority of the chemical has degraded. This is a result of the increased activity in the surface sediment layer due to both photolysis and anaerobic degradation processes at work, whereas subsurface residues are outside the photolytic zone.¹² Only microbial degradation processes are accounted for in the subsurface sediment layers. The model predicts small amounts of residues in the underlying sediment layer as a result of accounting for molecular diffusion through sediment pore gaps. Although the rate of movement of a highly sorptive compound such as etofenprox would be extremely slow, the short distance of the sediment layer 1 and 2 interface allows for downward movement into the sediment profile over the simulation time.

Etofenprox total water concentrations (bound and dissolved fraction) would be at a maximum of 0.72 ppb one day after application (levels below the LC₅₀ (2.5 ppb) of rainbow trout),²³ yet residues would remain above the no observable effects concentration (0.05 ppb; chronic reproduction toxicity test) for the sensitive aquatic invertebrate, *Daphnia magna*,²³ 22 days after application (Figure 4) if bioavailability is not considered. The release of field water with dissolved aqueous concentrations of etofenprox has the potential to cause adverse effects to the most sensitive species. Proper timing and rate of etofenprox application are crucial for the management of etofenprox residues and prevention of offsite movement of residues. Residues in the sediment will persist much longer, with an average sediment concentration of 51 ppb 100 days after application and more than twice the concentration of residues in sediment layer 2 compared to sediment layer 1 (Table 3). At this point in time, less than 5% is predicted to remain in the field. There are no ecotoxicity values for etofenprox residues in sediment available to compare the model output with. Soil erosion should be controlled, as etofenprox can be transported offsite in a bound state.

In comparison to etofenprox, malathion is much more water-soluble and reactive in the environment overall. The predicted dissipation profile for malathion is presented for the water, sediment, soil and air compartments in Figure 5. Malathion concentrations are greater than etofenprox initially as a result of the greater rate of application for malathion in all compartments. Due to its rapid degradation in water (Figure 5) and low sorption to sediments, malathion concentrations in the sediment are much lower than etofenprox sediment levels 100 days after application (Table 3). Based on the comparison of the percent decrease in mass remaining in the system over time, malathion is less persistent than etofenprox.

Sorbed etofenprox underwent photolytic transformation and degradation under simulated California summertime field light

Table 3. Model Predicted Environmental Concentrations 100 Days after Application

| compartment | etofenprox, ppb | malathion, ppb |
|-------------------|----------------------|----------------------|
| soil layer 1 | 1.6×10^0 | 2.4×10^{-3} |
| soil layer 2 | 5.9×10^0 | 6.3×10^{-5} |
| soil layer 3 | 3.3×10^{-1} | 2.6×10^{-7} |
| av soil concn | 1.5×10^0 | 8.1×10^{-4} |
| sediment layer 1 | 1.4×10^1 | 5.4×10^0 |
| sediment layer 2 | 8.2×10^1 | 6.6×10^0 |
| sediment layer 3 | 4.5×10^1 | 9.8×10^0 |
| av sediment concn | 5.1×10^1 | 7.3×10^0 |
| water | 4.2×10^{-4} | 2.4×10^{-2} |
| fish | 1.4×10^0 | 8.0×10^{-1} |
| vegetation | 2.7×10^{-3} | 3.4×10^{-3} |

intensity. The presence of floodwater enhanced the degradation rate of etofenprox on a soil surface. Due to the movement of residues to soils and solid surfaces after application, photodegradation is expected to dominate the dissipation of residues in a flooded field until rice plants begin to shade residues, at which point anaerobic microbial degradation will take over. The model simulation of etofenprox application suggests persistence of residues in the flooded soil at 100 days after application. The model is a useful tool to determine field management practices which prevent offsite movement of residues and persistence from a pest management perspective.

ASSOCIATED CONTENT

Supporting Information. Table of level IV fugacity model environmental input parameters, table of level IV fugacity model chemical and reaction rate input parameters, figure depicting predicted movement and dissipation profile of etofenprox and malathion within sediment layers 1, 2 and 3, and figure depicting predicted persistence of applied etofenprox and malathion. This material is available free of charge via the Internet at <http://pubs.acs.org>.

AUTHOR INFORMATION

Corresponding Author

*Tel: (530) 752-2534. Fax: (530) 752-3394. E-mail: mevasquez@ucdavis.edu.

Funding Sources

We wish to thank the California Rice Research Board (Grant #RP-7) for funding support.

ACKNOWLEDGMENT

We wish to thank P. Tomco for construction of the photoreactor; A. Van Scy, A. Tjeerdema, W. Yeung and C. Pan for laboratory and technical assistance; and Mitsui Chemicals, Inc., and Landis International Consulting for providing analytical standards and methods.

REFERENCES

- California Department of Pesticide Regulation. *Summary of pesticide use report data 2008; indexed by chemical*; California Environmental Protection Agency: Sacramento, CA, 2008; p 338. Available

online at <http://www.cdpr.ca.gov/docs/pur/pur08rep/chmrpt08.pdf> (accessed March 1, 2011).

(2) Weston, D. P.; You, J.; Lydy, M. J. Distribution and toxicity of sediment-associated pesticides in agriculture dominated water bodies of California's central valley. *Environ. Sci. Technol.* **2004**, *38*, 2752–2759.

(3) Class, T.; Casida, J.; Ruzo, L. Photochemistry of ethofenprox and three related pyrethroids with ether, alkane, and alkene central linkages. *J. Agric. Food Chem.* **1989**, *37*, 216–222.

(4) Vasquez, M.; Gunasekara, A.; Cahill, T.; Tjeerdema, R. Partitioning of etofenprox under simulated California rice field conditions. *Pest. Manage. Sci.* **2010**, *66*, 28–34.

(5) Vasquez, M.; Holstege, D. M.; Tjeerdema, R. Aerobic versus anaerobic microbial degradation of etofenprox in a California rice field soil. *J. Agric. Food Chem.* **2011**, *59*, 2486–2492.

(6) Katagi, T. Photodegradation of pesticides on plant and soil surfaces. *Rev. Environ. Contam. Toxicol.* **2004**, *182*, 1–195.

(7) University of California, Davis, Analytical Laboratory, College of Agricultural and Environmental Sciences, <http://anlab.ucdavis.edu/>; Accessed June 13, 2011.

(8) Sheldrick, B. H.; Wang, C. Particle-size distribution. In *Soil Sampling and Methods of Analysis*, Canadian Society of Soil Science; Carter, M. R., Ed.; Lewis Publishers: Ann Arbor, MI, 1993; pp 499–511.

(9) Nelson, D. W.; Sommers, L. E. Total carbon, organic carbon and organic matter. In *Methods of soil analysis: Part 2. Chemical and microbiological properties*; Page, A. L., et al., Eds.; ASA Monograph Number 9; American Society of Agronomy: Madison, WI, 1982; pp 539–579.

(10) Soil Survey Staff, Natural Resources Conservation Services, USDA. Soil survey of Butte area, California, parts of Butte and Plumas Counties, 2006. http://soildata.mart.nrccs.usda.gov/Manuscripts/CA612/0/Butte_CA.pdf (accessed June 22, 2010).

(11) Graebing, P.; Chib, J. S. Soil photolysis in a moisture- and temperature-controlled environment. 2. Insecticides. *J. Agric. Food Chem.* **2004**, *52*, 2606–2614.

(12) Cahill, T. M.; Mackay, D. Complexity in multimedia mass balance models: when are simple models adequate and when are more complex models necessary? *Environ. Toxicol. Chem.* **2003**, *22*, 1404–1412.

(13) Livezey, J.; Forman, L. Characteristics and production costs of US rice farms. USDA statistical bulletin # 974-7, March 2004.

(14) Texas Department of Agriculture. Pesticide Section 18 exemption Trebon on rice. Pesticide Programs Division (2006). Available online at: http://www.agr.state.tx.us/agr/main_render/0,1968,1848_5588_15087_0,00.html?channel=5588. (accessed June 13, 2011)

(15) California Department of Pesticide Regulation, *Summary of pesticide use report data 2006; indexed by commodity*; California Environmental Protection Agency: Sacramento, CA, 2008; p 316.

(16) Herbert, V. R.; Miller, G. C. Depth dependence of direct and indirect photolysis on soil surfaces. *J. Agric. Food Chem.* **1990**, *38*, 913–918.

(17) Ruggiero, P. Abiotic transformation of organic xenobiotics in soils: a compounding factor in the assessment of bioavailability. In *NATO Science Series 2. Environmental Security 64. Bioavailability of Organic Xenobiotics in the Environment*; NATO: Washington, DC, 1999; pp 159–205.

(18) Tsao, R.; Eto, M. Photolytic and chemical oxidation reactions of the insecticide etofenprox. *J. Pestic. Sci.* **1990**, *15*, 405–411.

(19) Katagi, T. Photodegradation of 3-phenoxybenzoic acid in water and on solid surfaces. *J. Agric. Food Chem.* **1992**, *40*, 1269–1274.

(20) Laskowski, D. Physical and chemical properties of pyrethroids. *Rev. Environ. Contam. Toxicol.* **2002**, *174*, 49–170.

(21) Tyler, C.; Beresford, N.; VanDer Woning, M.; Sumpter, J.; Thorpe, K. Metabolism and environmental degradation of pyrethroid insecticides produce compounds with endocrine activities. *Environ. Toxicol. Chem.* **2000**, *19*, 801–809.

(22) Laffin, B.; Chavez, M.; Pine, M. The pyrethroid metabolites 3-phenoxybenzoic acid and 3-phenoxybenzyl alcohol do not exhibit estrogenic activity in the MCF-7 human breast carcinoma cell line or Sprague-Dawley rats. *Toxicology* **2010**, *267*, 39–44.

(23) Report of the Joint Meeting of the FAO Panel of Experts on Pesticide Residues in Food and the Environment; World Health Organization: Geneva, Switzerland, September 20–29: 357–381 (1993).